Dual-Functional Gadolinium-Based Copper(II) Probe for Selective Magnetic Resonance Imaging and Fluorescence Sensing

Xiaolin Zhang,[†] Xu Jing,[†] Tao Liu,[†] Gang Han,[‡] Huaqiang Li,[†] and Chunying Duan*,[†]

[†]State Key Laboratory of Fine Chemicals, Dalian University of Technology, Dalian 116012, China
[‡]Department of Biochemistry and Molecular Pharmacology, University of Massachusetts Medical School, Worcester, Massachusetts 01605, United States

ABSTRACT: A unique gadolinium complex, **Nap-DO3A-Gd**, comprising a naphthylamine luminescent moiety, a di-2-picolyl-amine (DPA) binding chelator, and a 1,4,7,10-tetraazacyclododecane-1,4,7-triacetic acid (DO3A) moiety has been designed and synthesized as a dual-functional probe for selective magnetic resonance imaging and fluorescent sensing of copper(II) in living cells. **Nap-DO3A-Gd** exhibited a turn-on manner of relaxivity changes and a fluorescent quenching toward Cu^{2+}. Through the introduction of naphthalamide into the Gd^{3+} contrast agent platform to restrict the coordination ability of the DPA chelator and with Gd^{3+} coordinating to the DPA moiety to turn away the interferences of other metal cations from Cu^{2+} detection, the probe featured selective relaxivity changes toward Cu^{2+} over other metal ions and brought unique Cu^{2+}-specific luminescent responses. The probe was water-soluble with the luminescent detection limit established at 6 ppb and was successfully used for luminescence imaging detection of copper(II) in living cells. The results demonstrated the efficiency and advantage of our approach in the development of a dual-modality image.
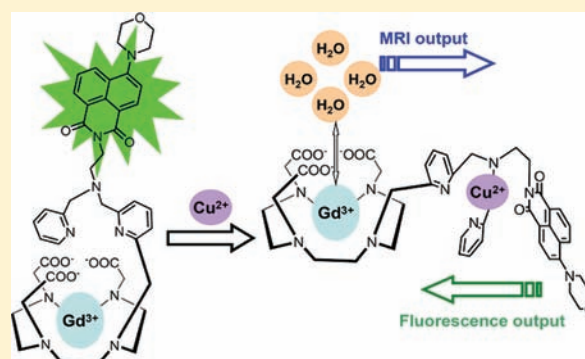
INTRODUCTION

Magnetic resonance imaging (MRI) has become increasingly popular in experimental molecular imaging and clinical because it is noninvasive and capable of producing three-dimensional representations of opaque organisms with high spatial and temporal resolution.[1−6] While the combination of metal-based MRI contrast agents with selective molecular recognition elements provides a promising new class of chemosensors for molecular imaging of essential s-block and d-block metal ions in biological systems, the quantitative measurements using MRI as a single modality are still challenging because the local concentration of the contrast agent is unknown, and the sensitivity of the MRI technique is relatively low compared to other modalities such as optical imaging or positron emission tomography.[7−18] In this regard, the attachment of a luminescent probe to an MRI contrast agent offers a potential powerful approach for the quantitative integration of molecular and cellular information about complex biological signaling networks at a system level because the fluorescent metal sensors exhibit excellent sensitivity and multiplexed detection capabilities at the cellular level and have been widely exploited in biotechnology and biomedical research fields.[19−25]

Of the transition-metal ions in the human body, copper is the third most abundant essential trace element. The alternations in its cellular homeostasis are connected to serious neuro-degenerative diseases including Alzheimer's disease, familial amyotrophic lateral sclerosis, Menkes and Wilson's diseases, and prion diseases.[26−28] Understanding the relationships

between copper regulation and its physiological or pathological consequences is fascinating and led to extensive interest in the development of new ways to study the aspects of copper-ion accumulation, trafficking, and export in living systems by live-cell optical imaging and MRI.[29−31] Because copper ions are involved in numerous molecular processes globally within an intact and complex whole body, rather than within an isolated in vitro system, the complementary nature of a dual-functional MRI/fluorescent emission probe that takes advantage of the exquisite sensitivity of optical techniques and the high spatial resolution of MRI methods will benefit the biological imaging copper ions.[32] Inspired by the elegant smart contrast agents for the β-galactosidase activity described by Meade et al.[1,4] and the synthetic approach of the naphthylamine-based probes for copper(II) ions,[33−35] herein, we reported a new approach to design and synthesize a dual-functional MRI/fluorescent emission probe through the incorporation of a Gd^{3+} contrast agent platform to a luminescent-active naphthylamine moiety having di-2-picolylamine (DPA) as a tridentate chelator. We envisioned that the DPA tridentate chelator coordinated to copper(II) strongly to relieve steric congestion around the Gd^{3+} center,[36−40] benefiting the increase of proton relaxivity. Also, the incorporation of a larger naphthylamine moiety will modify the coordination ability of DPA, from which the improvement

of the selectivity toward copper ions over other metal ions, especially for that of zinc(II) ions, is expected.

■ RESULTS AND DISCUSSION

Synthesis and Characterization of Nap-DO3A-Gd Probe. **Nap-DO3A-Gd** was synthesized according to the synthetic route outlined in Scheme 1. **3** was gained through the

Scheme 1. Synthetic Procedure for Nap-DO3A-Gd[a]
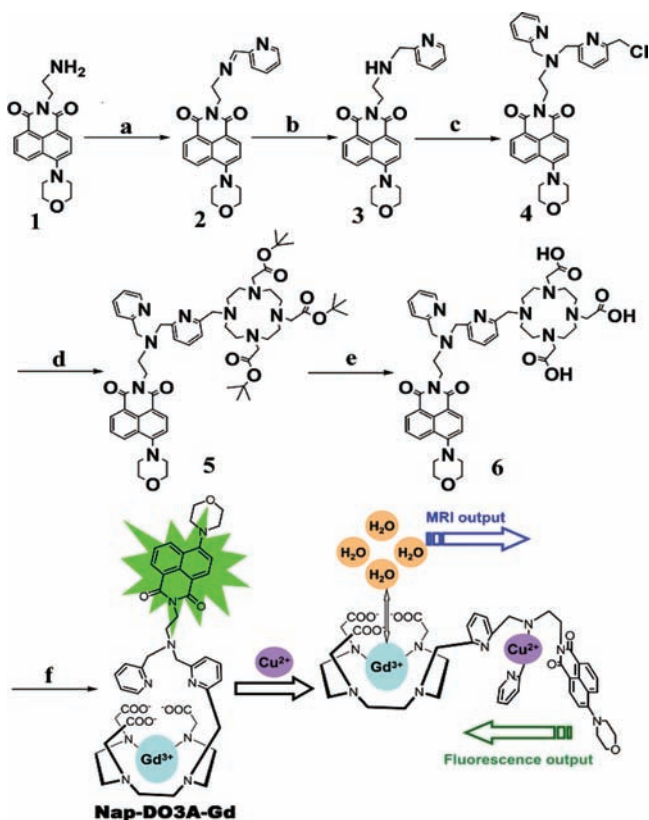
[a]Conditions: (a) 2-pyridinecarboxaldehyde, C_2H_5OH, reflux (83%); (b) sodium triacetoxyborohydride, CH_3OH, reflux (80%); (c) 2,6-bis(chloromethyl)pyridine, potassium carbonate, CH_3CN, reflux (60%); (d) tris*tert*-butyl ester of DO3A, $NaHCO_3$, CH_3CN, reflux (48%); (e) trifluoroacetic acid, CH_2Cl_2, rt (90%); (f) Gd-$(NO_3)_3 \cdot 6H_2O$, MeOH/H_2O, rt (51%).

Schiff base reaction and the reduction reaction of **1**. The nucleophilic substitution of bis(chloromethyl)pyridine with **3** gave **4** in a 60% yield. **4** was reacted with tri-*tert*-butyl ester of 1,4,7,10-tetraazacyclododecane-1,4,7-triacetic acid (DO3A) to produce **5** via alkylation. **5** was then treated with trifluoroacetic acid to remove the *tert*-butyl protecting groups and reacted overnight with Gd$(NO_3)_3 \cdot 6H_2O$. **Nap-DO3A-Gd** was purified via semipreparatory high-performance liquid chromatography (HPLC) on a reversed-phase column. Analytical HPLC–mass spectrometry (MS) was used to confirm the purity and identity of the collected fractions, and its Gd^{3+} content was analyzed using inductively coupled plasma optical emission spectroscopy (ICP-OES).

Electrospray MS (ESI-MS) of **Nap-DO3A-Gd** showed three peaks at m/z 511.04, 522.02, and 1021.32, assignable to $[H_2(\textbf{Nap-DO3A-Gd})]^{2+}$, $[NaH(\textbf{Nap-DO3A-Gd})]^{2+}$, and $[H-(\textbf{Nap-DO3A-Gd})]^{+}$, respectively (Figure 1). The addition of Cu^{2+} caused the disappearance of the peaks and brought out
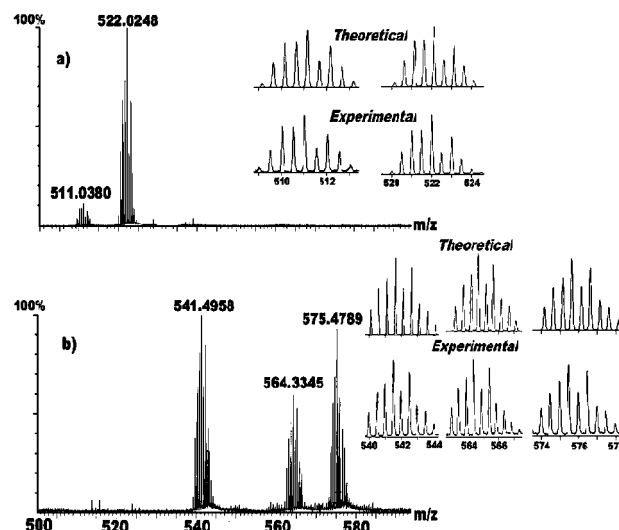
Figure 1. ESI-MS spectra of **Nap-DO3A-Gd** in the solution of methanol and water (1:2, v/v; m/z 500−600) in the absence of copper ions (a) and after the addition of copper ions (b). Insets: theoretical and experimental isotopic patterns at m/z 511.04, 522.02, 541.50, 564.33, and 575.48 in parts a and b.

three new peaks at m/z 541.50, 564.33, and 575.48. These peaks were assigned to $[Cu(\textbf{Nap-DO3A-Gd})]^{2+}$, $[Cu(\textbf{Nap-DO3A-Gd})(C_2H_5OH)]^{2+}$, and $[Cu(\textbf{Nap-DO3A-Gd})-(CH_3OH)(H_2O)_2]^{2+}$, respectively, according to the exact comparison of the intense peaks with the simulation on the basis of natural isotopic abundances. This result provides evidence of the formation of a 1:1 stoichiometric complexation species in solution. Upon the addition of zinc ions, instead of copper ions, no complexation species were detected in the ESI-MS spectra under the same experimental conditions, which suggests the better selectivity of **Nap-DO3A-Gd** to Cu^{2+} than Zn^{2+} in solution.

MRI Responses toward Cu^{2+}. The ability of Cu^{2+} to modulate the longitudinal relaxivity of **Nap-DO3A-Gd** was determined using T_1 measurements at a proton frequency of 20 MHz (pH 7.0; Figures 2 and 3). In the absence of Cu^{2+}, the
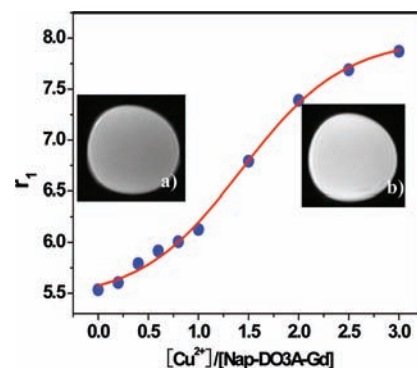
Figure 2. Relaxivity responses of **Nap-DO3A-Gd** (0.2 mM) to Cu^{2+} with various concentrations (T_1 measurements at a proton frequency of 20 MHz) and T_1-weighted phantom MRI images: (a) image of only **Nap-DO3A-Gd** (0.2 mM) in water; (b) image of **Nap-DO3A-Gd** (0.2 mM) and copper ions (0.6 mM) in water.

relaxivity of **Nap-DO3A-Gd** (0.2 mM) was 5.53 mM^{-1} s^{-1}, which gradually increased to 7.87 mM^{-1} s^{-1} with the addition of Cu^{2+} until 3 equiv of copper ions had been added. Adding
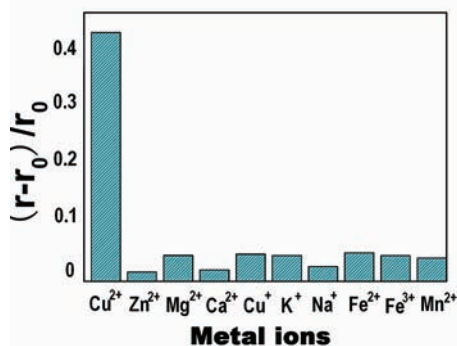
Figure 3. MRI responses (T_1 measurements at a proton frequency of 20 MHz) of **Nap-DO3A-Gd** (0.2 mM) upon the addition of metal ions of interest (0.6 mM).

Cu^{2+} triggered about 42% enhancement in the relaxivity. The observed relaxivity increases for **Nap-DO3A-Gd** are stable over time, indicating that $Gd^{3+}/DO3A$ has excellent stability and remains intact in the presence of Cu^{2+}.[14] The apparent K_A for the 1:1 Cu^{2+}/**Nap-DO3A-Gd** complex is 8.5×10^4 M^{-1}. Also, the acquired T_1-weighted images of **Nap-DO3A-Gd** (0.2 mM) with a commercial 0.5 T magnet in the absence and presence of copper ions (0.6 mM) readily visualized differences in the copper levels in a biologically relevant micromolar range.

The relaxivity changes of **Nap-DO3A-Gd** were Cu^{2+} specificity over other physiologically important metal ions including Ca^{2+}, Mg^{2+}, Na^+, K^+, Fe^{2+}, Fe^{3+}, Cu^+, and Mn^{2+}. Even upon the addition of 2 mM (10 equiv) of metal ions such as Ca^{2+}, Mg^{2+}, Na^+, and K^+, the relaxivity of **Nap-DO3A-Gd** hardly changed in an obvious manner. Interestingly, **Nap-DO3A-Gd** exhibited high excellent selectivity toward Cu^{2+} over Zn^{2+}; the addition of Zn^{2+} (0.6 mM) did not affect the relaxivity of **Nap-DO3A-Gd**. The better selectivity compared to the reported copper(II)-responsive MRI probes[37,38] is reasonably attributed to the introduction of naphthalimide into the Gd^{3+} contrast agent platform that restricts the coordination ability of the DPA chelator to that of zinc ions; only the ions exhibiting stronger binding ability could replace the Gd^{3+} ions to coordinate with the DPA donors. We also observed the MRI responses toward Cu^{2+} with a pH range from 5.5 to 8.0, and no significant variation was observed.

From a view of the mechanism, in the solution of a free **Nap-DO3A-Gd** probe, water molecules are limited in their inner-sphere access to the Gd^{3+} center by steric hindrance from the two bulky pyridine groups, which cap the **DO3A** moiety, therefore minimizing proton relaxivity. Upon binding Cu^{2+}, the Gd^{3+} ion is exposed to bulk water, thereby changing the relaxivity from weak to strong with DPA coordinated to the better acceptors of the copper ions. The fluorescence decay rates of the terbium(III) analogue in water and D_2O with and without copper(II) present were measured to calculate the number of inner-sphere water molecules (q; Table 1). The increase of q from 0.28 in the absence of Cu^{2+} to 2.58 after the addition of Cu^{2+} confirmed that Cu^{2+} binding to **Nap-DO3A-Gd** increases the number of the inner-sphere water molecules.[38–41]

Fluorescence Detection toward Cu^{2+}. Nap-DO3A-Gd displays a fluorescence band centered at 550 nm. Upon the addition of $Cu(NO_3)_2$ to the solution of **Nap-DO3A-Gd**, the fluorescence emission at 550 nm gradually decreased and then remained constant after the addition of approximately 1 equiv

Table 1. Luminescence Lifetimes (ms) and Calculated Number of Inner-Sphere Water Molecules (q) for Nap-DO3A-Tb (0.2 mM) in the Absence and Presence of Cu^{2+} (0.6 mM)^a

	τ_{H_2O}/ms	τ_{D_2O}/ms	q
Nap-DO3A-Tb	0.73	0.77	0.28
Nap-DO3A-Tb + Cu^{2+}	0.23	0.27	2.58

^{a}Luminescence measurements of the terbium(III) analogues were performed in the absence or presence of excess $Cu(NO_3)_2$. Samples were excited at 280 nm, and the emission maximum at 544 nm was used to determine luminescence lifetimes. The number of bound water molecules was estimated using Horrocks' equation:[39] $q = 4.2(1/\tau_{H_2O}/ms - 1/\tau_{D_2O}/ms)$, where τ is the luminescence lifetime in H_2O or D_2O.

of Cu^{2+} (Figure 4). Fitting of the fluorescence titration curve of **Nap-DO3A-Gd** (5 μM) revealed a 1:1 stoichiometry of the
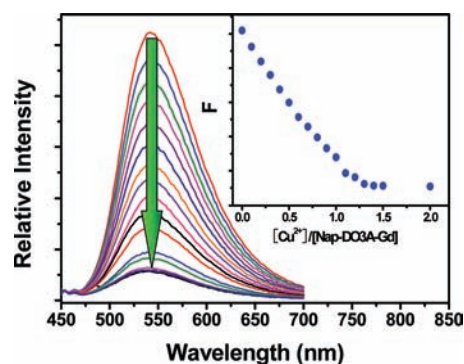
Figure 4. Family of fluorescence spectra of **Nap-DO3A-Gd** (5 μM, 1:2 CH_3OH/H_2O, pH 7.0) upon the addition of a $Cu(NO_3)_2$ aqueous solution. The intensity was recorded at 550 nm. Excitation at 400 nm. Inset: Titration profiles of **Nap-DO3A-Gd** upon the addition of Cu^{2+} showing fluorescence intensities at 550 nm.

Nap-DO3A-Gd/Cu^{2+} species with an association constant of 6.31×10^6 M^{-1}.[41] The related higher association constant calculated from the fluorescent titration than that from the MRI experiment might be due to the fact that the free copper ions also can induce the quench of fluorescence. The fluorescence quantum yield[42] decreased to 8% of the original one (from 0.054 to 0.0042) with EC_{50} (the concentration of Cu^{2+} in the case of the luminescence quench: 50%) being ca. 0.25 μM. Under optimized conditions, the fluorescence intensity of **Nap-DO3A-Gd** (0.1 μM) was nearly proportional to the copper concentration, with the detection limit about 6 ppb. Because the average concentration of blood copper in the normal group is 100−150 μg/L (15.7−23.6 μM),[43] **Nap-DO3A-Gd** thus is able to detect copper(II) in the normal physiological condition. Furthermore, the fluorescence quench of **Nap-DO3A-Gd** induced by Cu^{2+} could be recovered when a solution of glutathione was added. This indicated that the chelation of Cu^{2+} was reversible.

The fluorescence responses of **Nap-DO3A-Gd** (10 μM) exhibited excellent selectivity toward Cu^{2+} over other metal ions. No significant spectral changes were observed for **Nap-DO3A-Gd** (10 μM) in the presence of alkali- or alkaline-earth metals, such as Na^+, K^+, Mg^{2+}, and Ca^{2+} (Figure 5). Competition experiments revealed that the Cu^{2+}-induced fluorescence was unaffected in the presence of the metal
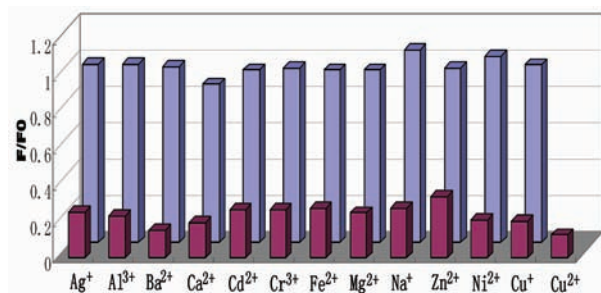
Figure 5. Fluorescence responses of **Nap-DO3A-Gd** (10 μM, 1:2 CH$_3$OH/H$_2$O, pH 7.0) to various metal ions with excitation wavelength at 400 nm. Blue bars represent the emission intensities of **Nap-DO3A-Gd** (10 μM) after the addition of the appropriate metal ions (10 μM Ag$^+$, Al^{3+}, Ba^{2+}, Cd^{2+}, Cr^{3+}, Fe^{2+}, Zn^{2+}, Ni^{2+}, Cu$^+$, and Cu^{2+} and 100 μM Mg^{2+}, Na$^+$, Ca^{2+}). Red bars represent the emission intensities that occur upon the subsequent addition of 10 μM Cu^{2+} to the above-mentioned solutions, respectively. Emission intensities were recorded at 550 nm, and the excitation wavelength was at 400 nm.

cations mentioned above. Interestingly, while DPA-functionalized naphthalimide-based probes exhibited zinc-specific fluorescence enhancement in aqueous media,[33−35] the fluorescence of **Nap-DO3A-Gd** was hardly affected by the presence of zinc ions, and the Cu^{2+}-induced fluorescent responses were also unaffected in the presence of zinc ions in solution. The excellent selectivity toward Cu^{2+} over zinc ions is attributed to the fact that the coordination of the DPA chelator to Gd^{3+} restricts the probe to complexate zinc ions; only the Cu^{2+} ions exhibiting stronger binding ability is able to replace the Gd^{3+} coordinating to the DPA donors. **Nap-DO3A-Gd** responded to Cu^{2+} in the pH range 5.5−8.0, with the fluorescence intensity varying by less than 10%, facilitating the detection of Cu^{2+} in aqueous media at physiological pH values.

Fluorescence imaging of intracellular Cu^{2+} was observed under a Nikon eclipse TE2000-5 inverted fluorescence microscope with a 20× objective lens. As shown by our fluorescence imaging experiments (Figure 6), staining of HeLa cells with a 10 μM solution of **Nap-DO3A-Gd** at room temperature for 30 min led to obvious intracellular green fluorescence. When cells stained with **Nap-DO3A-Gd** were incubated with 10 μM Cu^{2+} in phosphate-buffered saline (PBS; pH 7.4) for 30 min and washed, the obvious quenching of the fluorescence intensity was observed. The results indicate that cells were permeable to **Nap-DO3A-Gd** and copper ions could be detected in living cells.

In vivo experiments were also carried out to examine if **Nap-DO3A-Gd** could be used to detect Cu^{2+} in living organisms (Figure 7).[44] Five-day-old zebrafish were incubated with **Nap-DO3A-Gd** (10 μM) in PBS for 30 min and washed three times with PBS (pH 7.4). The obvious green fluorescence was observed and indicated that **Nap-DO3A-Gd** was successfully taken up into various organs of the zebrafish. However, the zebrafish incubated with **Nap-DO3A-Gd** (10 μM) and then treated with Cu^{2+} displayed a very weak fluorescence signal, indicating that copper ions in zebrafish were fluorescently detected by **Nap-DO3A-Gd**. These experiments show that **Nap-DO3A-Gd** can detect copper ions both in cultured cells and in whole organisms. For all images, the microscope settings, such as brightness, contrast, and exposure time, were held constant to compare the relative intensity of intracellular Cu^{2+} fluorescence.
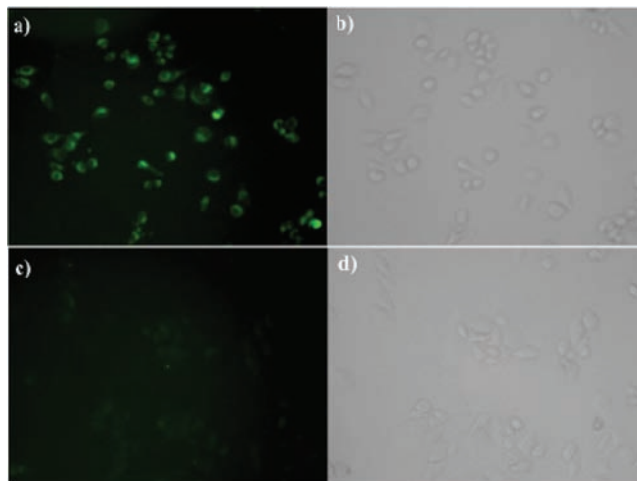
Figure 6. Fluorescence images of Cu^{2+} in HeLa cells: (a) Fluorescence image of HeLa cells incubated with **Nap-DO3A-Gd** (10 μM); (b) bright-field transmission image of HeLa cells incubated with **Nap-DO3A-Gd** (10 μM); (c) fluorescence image of HeLa cells incubated with **Nap-DO3A-Gd** for 15 min, washed three times, and further incubated with 10 μM Cu(NO$_3$)$_2$ for 15 min; (d) bright-field transmission image of HeLa cells incubated with **Nap-DO3A-Gd** (10 μM) and Cu(NO$_3$)$_2$ (10 μM).
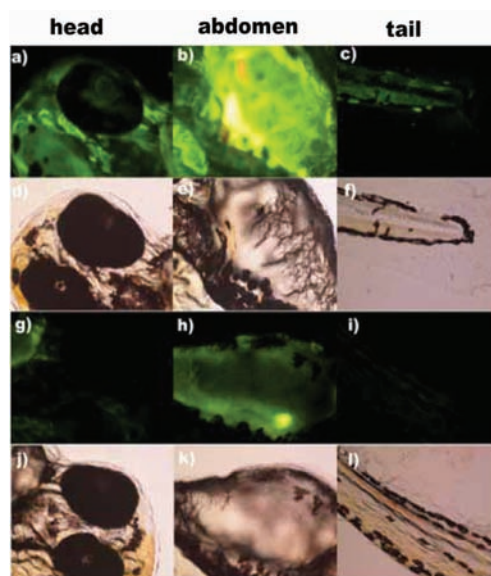
Figure 7. Fluorescence and bright-field images of a 5-day-old zebrafish incubated with **Nap-DO3A-Gd**: (a−c) fluorescence images of a zebrafish incubated with **Nap-DO3A-Gd** (10 μM); (d−f) bright-field images of a zebrafish from panels a−c; (g−i) fluorescence images of a zebrafish incubated with **Nap-DO3A-Gd** (10 μM) and further incubated with Cu^{2+} (10 μM); (j−l) bright-field images of a zebrafish from panels g−i. Excited with blue light (400−460 nm).

■ CONCLUSIONS

In conclusion, we designed and synthesized a dual-modality MRI and fluorescent copper-specific probe in aqueous solution. **Nap-DO3A-Gd** exhibited a turn-on manner of relaxivity changes and a fluorescent quenching toward Cu^{2+}. It provides the possibility of its application as the dual-modality probe in biological systems. Through the introduction of bulky naphthalimide into the Gd^{3+} contrast agent platform to restrict the coordination ability of the DPA chelator, the relaxivity

changes of **Nap-DO3A-Gd** showed excellent selectivity toward Cu^{2+} over other metal ions, especially for that of Zn^{2+}. Also, with the Gd^{3+} coordinated to the DPA moiety to turn away the interferences of other metal cations from Cu^{2+} detection, the luminescence responses were Cu^{2+}-specific.

■ EXPERIMENTAL SECTION

Instruments and Reagents. All reagents and solvents were of analytical reagent grade and were used without further purification. 2-Pyridinecarboxaldehyde, 1,4,7,10-tetraazacyclododecane(cyclen), and sodium triacetoxyborohydride were purchased from Sigma-Aldrich. Metal salts were provided by Shanghai Fourth Chemical Reagent Company (China). Thin-layer chromatography was performed on silica gel 60F-254 glass plates. Reaction products were purified by flash chromatography using silica gel. Reversed-phase chromatography was performed by Dalian Zhonghuida Scientific Instrument Company using C18 columns. ^1H and ^{13}C NMR spectra were measured on a Varian INOVA 400 M spectrometer. ESI-MS analyses were carried out on a HPLC-Q-Tof MS spectrometer using methanol as the mobile phase. Fluorescence spectra of solutions were measured on an Edinburgh FS920 spectrometer. ICP-OES was performed on a Perkin-Elmer Optima 2000 DV ICP-OES. NMR imaging was performed on an NMR NMI20-Analyst Analyzing & Imaging system (Shanghai Niumag Corp.) using a 0.5 T magnet, point resolution = 256 × 128 mm, section thickness = 2 mm, TE = 23 ms, TR = 500 ms, and number of acquisitions = 4.

General Procedure for Detecting Spectra. Stock solutions (10^{-3} M) of **Nap-DO3A-Gd** were prepared in water (pH 7.0). Stock solutions (10^{-2} M) of nitrate salts of various metal ions of Na^+, Ca^{2+}, Mg^{2+}, Cu^{2+}, Zn^{2+}, Cd^{2+}, Al^{3+}, Fe^{3+}, Cr^{3+}, Ba^{2+}, Ag^+, and Ni^{2+} and sulfate salts of Fe^{2+} were prepared in water for spectrometric analysis. Cu^{2+} fluorescence was titrated at an excitation wavelength of 400 nm. Before spectroscopic measurements, solutions were freshly prepared by diluting the corresponding high-concentration stock solution. For each spectrum, 2 mL of a probe solution was added to a 1-cm quartz cell, to which different stock solutions of cations were gradually added using a microsyringe. The added volume of a cationic stock solution was always less than 100 μL to minimize changes in the total volume of the testing solution. Fluorescence quantum yield was determined using rhodamine B (Φ_f = 0.69 in ethanol) as the standard.[42] All spectroscopic measurements were performed at least in triplicate and averaged. Also, the quantum yield was calculated using equation

$$\Phi_{unk} = \Phi_{std} \frac{(I_{unk}/A_{unk})}{(I_{std}/A_{std})} \left(\frac{\eta_{unk}}{\eta_{std}}\right)^2$$

where Φ_{unk} and Φ_{std} are the radiative quantum yields of the sample and standard, I_{unk} and I_{std} are the integrated emission intensities of the corrected spectra for the sample and standard, A_{unk} and A_{std} are the absorbances of the sample and standard at the excitation wavelength, and η_{unk} and η_{std} are the indices of refraction of the sample and standard solutions, respectively. Excitation and emission slit widths were modified to adjust the luminescent intensity in a suitable range.

Fluorescence Microscopy Imaging in Cultured Cells and Zebrafish. Fluorescence images were observed under a Nikon eclipse TE2000-5 inverted fluorescence microscope with a 20× objective lens excited with blue light (400−460 nm). For all images, the microscope settings, such as brightness, contrast, and exposure time, were held constant to compare the relative intensities of intracellular Cu^{2+} fluorescence.

HeLa cell incubation and imaging HeLa cells were cultured at 37 °C in a 1640 medium supplemented with 10% FCS (Invitrogen). Cells were seeded in 24-well flat-bottomed plates. After 12 h, HeLa cells were incubated with 10 μM **Nap-DO3A-Gd** (in a culture medium) for 30 min at room temperature, washed three times with PBS, incubated with 10 μM Cu^{2+} for another 30 min, and rinsed three times with PBS. These HeLa cells were subjected to fluorescence imaging of intracellular Cu^{2+}.

Zebrafish incubation and imaging zebrafish were maintained at 28 °C. For mating, male and female zebrafish were maintained in one tank on a 12 h light/12 h dark cycle. Egg spawning was triggered by light stimulation in the morning. Almost all eggs were fertilized immediately. Five-day-old zebrafish were maintained in an E3 embryo medium (15 mM NaCl, 0.5 mM KCl, 1 mM $MgSO_4$, 1 mM $CaCl_2$, 0.15 mM KH_2PO_4, 0.05 mM Na_2HPO_4, 0.7 mM $NaHCO_3$, and 10^{-5}% methylene blue; pH 7.5). The 5-day-old zebrafish were incubated in an E3 medium containing 10 μM **Nap-DO3A-Gd** for 30 min at room temperature. After washing three times with PBS to remove the remaining **Nap-DO3A-Gd** in solution, the zebrafish were further incubated in solution containing 10 μM Cu^{2+} for 30 min at room temperature. These zebrafish were imaged by fluorescence microscopy.

Synthesis of Compound 1. To a solution of 4-bromoanhydride naphthalene (5 g, 18.2 mmol) in ethylene glycol monomethyl ether was added morpholine (4.74 g, 54.3 mmol). After 4 h under reflux conditions, the reaction was cooled to room temperature and yellow needle crystals were filtered. Crude product (4-morpholinoanhydride naphthalene) was used directly without further purification. To a solution of ethylenediamine (4.2 g, 70 mmol) in ethanol was added 4-morpholinoanhydride naphthalene (2 g, 7 mmol), and the resulting mixture was refluxed for 2 h. The reaction was cooled to room temperature and concentrated via rotary evaporation. The crude product was purified on a silica gel column, eluting with 10% methanol in dichloromethane. Compound **1** was collected in 60% yield as an orange solid. R_f = 0.5 [SiO_2; 9:1 (v/v) dichloride/methanol]. ^1H NMR (400 MHz, DMSO-d_6): δ 8.32−8.49 (m, 3H, ArH), 7.80 (t, 1H, J = 8.0 Hz, ArH), 7.34 (d, 1H, J = 8.0 Hz, ArH), 4.04 (t, 2H, J = 8.0 Hz, −CH_2CH_2−), 3.91 (t, 4H, J = 4.0 Hz, −CH_2CH_2−), 2.50−3.21 (m, 8H, 4H for −CH_2CH_2, −2H for −CH_2CH_2−, 2H for −NH_2). ^{13}C NMR (100 MHz, DMSO-d_6): δ 164.2, 163.7, 155.8, 132.5, 131.0, 130.9, 129.6, 126.5, 125.7, 123.2, 116.6, 115.5, 79.6, 66.7, 53.5, 43.1. TOF-ESI-MS. Calcd for [$C_{18}H_{19}N_3O_3$ + H]$^+$: m/z 326.1505. Found: m/z 326.1508.

Synthesis of Compound 2. Compound **1** (1 g, 3 mmol) was dissolved in ethanol with 2-pyridinecarboxaldehyde (0.39 g, 3.6 mmol). The reaction was stirred and refluxed for 6 h. The yellow solid was precipitated, and the reaction was cooled to room temperature and filtered. Compound **3** was obtained as a yellow powder. Yield: 1.26 g, 83%. R_f = 0.3 [SiO_2; 40:1 (v/v) dichloride/methanol]. ^1H NMR (400 MHz, CDCl$_3$): δ 8.60 (m, 2H, 1H for −N═CH−, 1H for ArH), 8.54 (d, 1H, J = 8.0 Hz, ArH), 8.42 (m, 2H, ArH), 7.99 (d, 1H, J = 8.0 Hz, ArH), 7.21 (m, 2H, ArH), 7.26−7.30 (m, 2H, ArH), 4.58 (t, 2H, J = 8.0 Hz, −CH_2CH_2−), 4.01−4.05 (m, 6H), 3.27 (t, 4H, J = 4.0 Hz, −CH_2CH_2−). ^{13}C NMR (100 MHz, CDCl$_3$): δ 164.4, 163.9, 163.3, 155.7, 154.5, 149.3, 136.6, 132.6, 130.2, 130.1, 129.9, 126.1, 125.8, 124.7, 123.2, 121.4, 117.1, 114.9, 67.0, 58.6, 53.4, 40.4. TOF-ESI-MS. Calcd for [$C_{24}H_{22}N_4O_3$ + H]$^+$: m/z 415.1770. Found: m/z 415.1785.

Synthesis of Compound 3. Sodium triacetoxyborohydride (1.5 g, 7.2 mmol) was added to a solution of compound **2** (1 g, 2.4 mmol) in methanol and refluxed for 2 h. Then the reaction mixture was cooled to room temperature. After concentration under reduced pressure, the mixture was poured into a KOH solution and extracted with dichloromethane, dried over $MgSO_4$, and evaporated under reduced pressure. The crude product **3** was purified on flash silica gel using dichloromethane/methanol (40:1) as the eluent. Yield: 0.8 g, 80%. R_f = 0.5 [SiO_2; 40:1 (v/v) dichloride/methanol]. ^1H NMR (400 MHz, CDCl$_3$): δ 8.59 (d, 1H, J = 8.0 Hz, ArH), 8.53 (d, 1H, J = 8.0 Hz, ArH), 8.49 (d, 1H, J = 8.0 Hz, ArH), 8.42 (d, 1H, J = 8.0 Hz, ArH), 7.71 (d, 1H, J = 8.0 Hz, ArH), 7.58 (d, 1H, J = 8.0 Hz, ArH), 7.30 (d, 1H, J = 8.0 Hz, ArH), 7.23 (d, 1H, J = 8.0 Hz, ArH), 7.11 (t, 1H, J = 8.0 Hz, ArH), 4.39 (t, 2H, J = 6.0 Hz, −CH_2CH_2−), 4.00−4.03 (m, 6H, 4H for −CH_2CH_2−, 2H for −CH_2−), 3.27 (t, 4H, J = 4.0 Hz, −CH_2CH_2−), 3.06 (t, 2H, J = 6.0 Hz, −CH_2CH_2−). ^{13}C NMR (100 MHz, CDCl$_3$): δ 164.6, 164.2, 159.6, 155.7, 149.3, 136.4, 132.6, 131.3, 130.1, 130.0, 126.2, 125.8, 123.3, 122.3, 121.9, 117.2, 115.0, 67.0, 54.8, 53.5, 47.4, 39.8. TOF-ESI-MS. Calcd for [$C_{24}H_{24}N_4O_3$ + H]$^+$: m/z 417.1927. Found: m/z 417.1941.

Synthesis of Compound 4. 2,6-Bis(chloromethyl)pyridine was synthesized as described.[45] Benzoyl peroxide (1.25 g, 4.65 mmol) was added in batches to a solution of 2,6-dimethylpyridine (10 g, 0.093 mol) and N-chlorosuccinimide (24.8 g, 0.186 mol) in carbon tetrachloride. The reaction was refluxed for 24 h until the raw material was consumed completely. The mixture was cooled to room temperature and filtered. The solvent was evaporated under reduced pressure. The crude product was purified on flash silica gel using CH_2Cl_2/petroleum ether (1:1, v/v) as the eluent to yield a white solid [2,6- bis(chloromethyl)pyridine]. ^1H NMR (400 MHz, $CDCl_3$): δ 7.77 (t, 1H, J = 7.6 Hz, ArH), 7.44 (d, 2H, J = 7.6 Hz, ArH), 4.67 (s, 4H, $-CH_2-$). ^{13}C NMR (100 MHz, $CDCl_3$): δ 156.4, 138.2, 122.1, 46.4. The solution of compound 3 (600 mg, 1.44 mmol) in acetonitrile was slowly added to a solution of 6-bis(chloromethyl)pyridine (757 mg, 4.32 mmol) and potassium carbonate (796 mg, 5.76 mmol) in acetonitrile. The reaction mixture was stirred and refluxed for 8 h. After the solvent was evaporated under reduced pressure, the crude product was purified by silica gel column chromatography using CH_2Cl_2/MeOH (50:1, v/v) as the eluent to afford a yellow solid. Yield: 480 mg, 60%. R_f = 0.50 [SiO_2; 50/1 (v/v) dichloride/methanol]. ^1H NMR (400 MHz, $CDCl_3$): δ 8.52 (d, 1H, J = 8.0 Hz, ArH), 8.41−8.51 (m, 3H, ArH), 7.72 (d, 1H, J = 8.0 Hz, ArH), 7.38 (d, 1H, J = 8.0 Hz, ArH), 7.29−7.31 (m, 3H, ArH), 7.24 (d, 1H, J = 8.0 Hz, ArH), 7.18 (d, 1H, J = 4.0 Hz, ArH), 7.01 (d, 1H, J = 4.0 Hz, ArH), 4.55 (s, 2H, $-CH_2-$), 4.40 (t, 2H, J = 6.0 Hz, $-CH_2CH_2-$), 4.04 (t, 4H, J = 6.0 Hz, $-CH_2CH_2-$), 3.93 (s, 2H, $-CH_2-$), 3.90 (s, 2H, $-CH_2-$), 3.30 (t, 4H, J = 6.0 Hz, $-CH_2CH_2-$), 2.94 (t, 2H, J = 6.0 Hz, $-CH_2CH_2-$). ^{13}C NMR (100 MHz, $CDCl_3$): δ 164.2, 163.7, 159.7, 155.6, 148.8, 137.0, 136.1, 132.5, 131.1, 130.0, 129.9, 126.1, 125.9, 123.4, 122.8, 122.0, 121.7, 120.6, 117.3, 115.0, 67.0, 60.4, 60.1, 53.5, 51.8, 46.7, 37.9. TOF-ESI-MS. Calcd for $[C_{31}H_{30}ClN_5O_3 + H]^+$: m/z 556.2115. Found: m/z 556.2123.

Synthesis of Compound 5. Tri-tert-butyl ester of 1,4,7,10-tetraazacyclododecane-1,4,7-triacetic acid (DO3A) was synthesized as described.[46] To the solution of cyclen (1 g, 5.8 mmol) in acetonitrile was slowly added dry sodium bicarbonate (1.95 g, 4.0 equiv) and bromoacetic acid/tert-butyl ester (3.74 g, 19.1 mmol, 3.3 equiv) in an ice bath. Then the mixture was stirred for 18 h and filtered. The filtrate was evaporated to dryness. The crude product was recrystallized from toluene. Compound 4 (400 mg, 0.72 mmol) and tri-tert-butyl ester of DO3A (370 mg, 0.72 mmol) were dissolved in acetonitrile (50 mL) under argon. An excess of $NaHCO_3$ (242 mg, 2.88 mmol) was added to the solution. The mixture was refluxed for 8 h and filtered, and the solvent was evaporated. The residue was purified using silica gel column chromatography, eluting with dichloromethane/methanol (40:1) to give 5 as a pale-yellow solid. Yield: 360 mg, 48%. R_f = 0.20 [SiO_2; 30/1 (v/v) dichloride/methanol]. ^1H NMR (400 MHz, $CDCl_3$): δ 8.42−8.48 (m, 4H, ArH), 7.77 (d, 1H, J = 8.0 Hz, ArH), 7.52 (d, 1H, J = 8.0 Hz, ArH), 7.46 (m, 2H, ArH), 7.30 (d, 1H, J = 8.0 Hz, ArH), 7.17 (d, 1H, J = 8.0 Hz, ArH), 7.02−7.10 (m, 2H, ArH), 4.35 (t, 2H, J = 6.4 Hz, $-CH_2-$), 4.05 (t, 4H, J = 4.8 Hz, $-CH_2-$), 4.00 (s, 2H), 3.79 (s, 2H), 3.77 (s, 2H), 3.64 (m, 4H), 3.36 (s, 4H), 3.32 (t, 4H, J = 4.8 Hz, $-CH_2-$), 3.15 (br, 4H), 2.91−2.95 (m, 12H), 1.47 (s, 9H), 1.43 (s, 18H). ^{13}C NMR (100 MHz, $CDCl_3$): δ 172.9, 172.2, 164.0, 163.6, 160.8, 159.8, 156.8, 155.7, 148.7, 137.2, 136.0, 132.4, 131.1, 130.2, 129.8, 126.1, 126.0, 123.3, 122.5, 122.4, 122.0, 121.7, 117.1, 115.0, 82.4, 82.1, 67.0, 60.9, 60.7, 60.0, 56.7, 56.1, 53.5, 52.0, 51.6, 50.6, 50.4, 37.8, 28.2, 28.1, 28.0. TOF-ESI-MS. Calcd for $[C_{57}H_{79}N_9O_9 + H]^+$: m/z 1034.6079. Found: m/z 1034.6075.

Synthesis of Compound 6. To a solution of compound 5 (200 mg, 0.19 mmol) in CH_2Cl_2 was added dropwise a solution of trifluoroacetic acid (1.5 mL) in CH_2Cl_2 (2 mL). The resulting solution was stirred for 24 h, and the solvent was removed by rotary evaporation. The residue was washed with cold ethyl ether (3 × 10 mL), and the solid was filtered to yield compound 6 as a yellow solid. Yield: 150 mg, 90%. ^1H NMR (400 MHz, CD_3OD): δ 8.61 (d, 1H, J = 8.4 Hz, ArH), 8.52 (d, 1H, J = 7.2 Hz, ArH), 8.44−8.48 (m, 2H, ArH), 7.98 (t, 1H, J = 7.2 Hz, ArH), 7.83 (t, 1H, J = 7.8 Hz, ArH), 7.74 (m, 2H, ArH), 7.54 (m, 2H, ArH), 7.40 (m, 2H, ArH), 4.48−4.51 (m, 4H), 4.38 (s, 2H), 4.24 (s, 2H), 4.03 (s, 4H), 3.86 (s, 2H), 3.24−3.62 (m, 26H). TOF-ESI-MS. Calcd for $[C_{45}H_{55}N_9O_9 + H]^+$: m/z 866.4201. Found: m/z 866.4203.

Synthesis of Nap-DO3A-Gd. $Gd(NO_3)_3 \cdot 6H_2O$ (32 mg, 0.086 mmol) and compound 6 (50 mg, 0.057 mmol) were combined in a solution of methanol and water (1:1, v/v). The pH was adjusted to 6−7 with added portions of dilute aqueous NaOH, and the reaction was stirred at room temperature overnight, maintaining the solution at pH 6−7 with added portions of NaOH. The solvent was removed by rotary evaporation, and the crude product was purified by reversed-phase C_{18} chromatography, eluting with MeOH/H_2O to yield a yellow solid (30 mg, 51%). The purity and identity of the collected fractions were confirmed by analytical HPLC−MS. The Gd content was measured using ICP-OES. TOF-ESI-MS. Calcd for $[M + H^+]$: m/z 1021.3. Found: m/z 1021.3. The appropriate isotope distribution was observed.

Synthesis of Nap-DO3A-Tb. **Nap-DO3A-Tb** was synthesized in a manner analogous to that of **Nap-DO3A-Gd** using $Tb(NO_3)_3 \cdot 6H_2O$. The purity and identity of the collected fractions were confirmed by analytical HPLC−MS. TOF-ESI-MS. Calcd for $[M + H^+]$: m/z 1022.3. Found: m/z 1022.2. Calcd for $[M + Na^+]$: m/z 1044.3. Found: m/z 1044.2. The appropriate isotope distribution was observed.

■ AUTHOR INFORMATION

Corresponding Author

*E-mail: cyduan@dlut.edu.cn.

Notes

The authors declare no competing financial interest.

■ ACKNOWLEDGMENTS

■ REFERENCES

(1) Moats, R. A.; Fraser, S. E.; Meade, T. J. Angew. Chem., Int. Ed. 1997, 36, 726−728.

(2) Caravan, P. Chem. Soc. Rev. 2006, 35, 512−523.

(3) Esqueda, A. C.; López, J. A.; Andreu-de-Riquer, G.; Alvarado-Monzón, J. C.; Ratnakar, J.; Lubag, A. J. M.; Sherry, A. D.; De León-Rodriguez, L. M. J. Am. Chem. Soc. 2009, 131, 11387−11391.

(4) Louie, A. Y.; Huber, M. M.; Ahrens, E. T.; Rothbacher, U.; Moats, R.; Jacobs, R. E.; Fraser, S. E.; Meade, T. J. Nat. Biotechnol. 2000, 18, 321−325.

(5) Woods, M.; Woessner, D. E.; Sherry, A. D. Chem. Soc. Rev. 2006, 35, 500−511.

(6) Rodriguez, L. M. D.; Lubag, A. J. M.; Malloy, C. R.; Martinez, G. V.; Gillies, R. J.; Sherry, A. D. Acc. Chem. Res. 2009, 42, 948−957.

(7) Trokowski, R.; Zhang, S.; Sherry, A. D. Bioconjugate Chem. 2004, 15, 1431−1440.

(8) Liu, G.; Li, Y.; Pagel, M. D. Magn. Reson. Med. 2007, 58, 1249−1256.

(9) Mizukami, S.; Takikawa, R.; Sugihara, F.; Hori, Y.; Tochio, H.; Walchli, M.; Shirakawa, M.; Kikuchi, K. J. Am. Chem. Soc. 2008, 130, 794−795.

(10) Trokowski, R.; Ren, J.; Kálmán, F. K.; Sherry, A. D. Angew. Chem., Int. Ed. 2005, 44, 6920−6923.

(11) Dhingra, K.; Maier, M. E.; Beyerlein, M.; Angelovski, G.; Logothetis, N. K. Chem. Commun. 2008, 29, 3444−3446.

(12) Major, J. L.; Boiteau, R. M.; Meade, T. J. Inorg. Chem. 2008, 47, 10788−10795.

(13) Datta, A.; Hooker, J. M.; Botta, M.; Francis, M. B. J. Am. Chem. Soc. 2008, 130, 2546−2552.

(14) Li, W. H.; Fraster, S. E.; Meade, T. J. J. Am. Chem. Soc. 1999, 121, 1413−1414.

(15) Trokowski, R.; Ren, J.; Kálmán, K.; Sherry, A. D. Angew. Chem., Int. Ed. 2005, 44, 6920−6923.

(16) Livramento, J. B.; Tóth, É.; Sour, A.; Borel, A.; Merbach, A. E.; Ruloff, R. *Angew. Chem., Int. Ed.* **2005**, *44*, 1480−1484.

(17) Ruloff, R.; Koten, G. V.; Merbach, A. E. *Chem. Commun.* **2004**, 842−843.

(18) Major, J. L.; Parigi, G.; Luchinat, C.; Meade, T. J. *Proc. Natl. Acad. Sci. U.S.A.* **2007**, *104*, 13881−13886.

(19) Zhang, X. A.; Lovejoy, K. S.; Jasanoff, A.; Lippard, S. J. *Proc. Natl. Acad. Sci. U.S.A.* **2007**, *104*, 10780−10785.

(20) You, Y.; Tomat, E.; Hwang, K.; Atanasijevic, T.; Nam, W.; Jasanoff, A. P.; Lippard, S. J. *Chem. Commun.* **2010**, *46*, 4139−4141.

(21) Haugland, R. P. *Handbook of Fluorescent Probes and Research Products*, 9th ed.; Molecular Probes: Eugene, OR, 2002.

(22) Tu, C.; Nagao, R.; Louie, A. Y. *Angew. Chem., Int. Ed.* **2009**, *48*, 6547−6551.

(23) Hüber, M. M.; Staubli, A. B.; Kustedjo, K.; Gray, M. H. B.; Shih, J.; Fraster, S. E.; Jacobs, R. E.; Meade, T. J. *Bioconjugate Chem.* **1998**, *9*, 242−249.

(24) Weissleder, R.; Pittet, M. J. *Nature* **2008**, 580−589.

(25) Chou, S. W.; Shau, Y. H.; Wu, P. C.; Yang, Y. S.; Shieh, D. B.; Chen, C. C. *J. Am. Chem. Soc.* **2010**, *132*, 13270−13278.

(26) Brewer, G. J. *Chem. Res. Toxicol.* **2010**, *23*, 319−326.

(27) Strausak, D. *Brain. Res. Bull.* **2001**, *55*, 175−185.

(28) Huang, J. H.; Xu, Y. F.; Qian, X. H. *Dalton Trans.* **2009**, 1761−1766.

(29) Que, E. L.; Domaille, D. W.; Chang, C. J. *Chem. Rev.* **2008**, *108*, 1517−1549.

(30) Tisato, F.; Marzano, C.; Porcbia, M.; Pellei, M.; Santini, C. *Med. Res. Rev.* **2010**, *30*, 708−749.

(31) Li, W. S.; Luo, J.; Chen, Z. N. *Dalton Trans.* **2010**, *40*, 484−488.

(32) Cheon, J.; Lee, J. H. *Acc. Chem. Res.* **2008**, *41*, 1630−1640.

(33) Wang, J. B.; Xiao, Y.; Zhang, Z. C.; Qian, X. H.; Yang, Y. Y.; Xu, Q. *J. Mater. Chem.* **2005**, *15*, 2836−2839.

(34) Kim, S. Y.; Hong, J. I. *Tetrahedron Lett.* **2009**, *50*, 2822−2824.

(35) Chen, X. Q.; Jou, M. J.; Yoon, J. Y. *Org. Lett.* **2009**, *11*, 2181−2184.

(36) Que, E. L.; Gianolio, E.; Baker, S. L.; Wong, A. P.; Aime, S.; Chang, C. J. *J. Am. Chem. Soc.* **2009**, *131*, 8527−8536.

(37) Que, E. L.; Chang, C. J. *J. Am. Chem. Soc.* **2006**, *128*, 15942−15943.

(38) Que, E. L.; Chang, C. J. *Chem. Soc. Rev.* **2010**, *39*, 51−60.

(39) Horrocks, W. D. Jr.; Sudnick, D. R. *Acc. Chem. Res.* **1981**, *14*, 384−392.

(40) Que, E. L.; Gianolio, E.; Baker, S. L.; Aime, S.; Chang, C. J. *Dalton Trans.* **2010**, *39*, 469−476.

(41) Connors, K. A. *Binding Contants*; John Wiley: New York, 1987.

(42) Olmsted, J. *J. Phys. Chem.* **1979**, *83*, 2581−2584.

(43) Tak, W. T.; Yoon, S. C. *Korean J Nephrol* **2001**, *20*, 863.

(44) Ko, S. K.; Chen, X. Q.; Yoon, J. Y.; Shin, I. *Chem. Soc. Rev.* **2011**, *40*, 2120−2130.

(45) Newkome, G. R.; Kiefer, G. E.; Xia, Y. J.; Gupta, V. K. *Synthesis* **1984**, *8*, 676−679.

(46) Mizukami, S.; Tonai, K.; Kaneko, M.; Kikuchi, K. *J. Am. Chem. Soc.* **2008**, *130*, 14376−14377.